

AdS/CFT aspects of the cosmological QCD phase transition

Cong-Xin Qiu*

Department of Astronomy, Nanjing University, Nanjing, Jiangsu 210093, People's Republic of China

(Received 18 December 2008; published 6 March 2009)

Recently, deeper understanding of QCD emerges from the study of the AdS/CFT correspondence. New results include the properties of quark-gluon plasma and the confinement/deconfinement phase transition, which are both very important for the scenario of the QCD phase transition in the early universe. In this paper, we study some aspects of how the new results may affect the old calculations of the cosmological QCD phase transition, which are mainly based on the studies of perturbative QCD, lattice QCD, and the MIT bag model.

DOI: [10.1103/PhysRevD.79.063505](https://doi.org/10.1103/PhysRevD.79.063505)

PACS numbers: 98.80.Cq, 11.25.Tq, 25.75.Nq

I. INTRODUCTION

Phase transitions can produce relics, affect the anisotropies of the universe, or have other observable consequences; hence, it is very important in astrophysics. A particularly important phase transition is the QCD confinement/deconfinement phase transition, in which the deconfined quark-gluon plasma (QGP) phase transits to the confined hadronic phase. By assuming this phase transition is first order and that it has nonzero surface tension, it suffers chronologically the processes of supercooling, reheating, bubble nucleation, and may produce relics such as quark nuggets. For the up to date reviews of the cosmological QCD phase transition, see [1,2].

Recently, deeper understanding of QCD emerges from the study of the anti-de Sitter/conformal field theory (AdS/CFT) correspondence [3]. In its prototype version, type IIB superstring theory on $\text{AdS}_5 \times S^5$ is dual to $\mathcal{N} = 4$ $U(N_c)$ super Yang-Mills (SYM) theory in $(3 + 1)$ -dimensional spacetime [4]. Generally speaking, conventional quantum field theories make sense only in the perturbative regions, where the 't Hooft coupling $\lambda_4 = g_{\text{YM}}^2 N_c$ is small; however, the dual gravity theory is easy to handle when the supergravity (SUGra) description becomes reliable, that is, in the strong coupling region. Hence, we can use the AdS/CFT correspondence to study field theory in the region where perturbative approaches are not applicable. It is also believed that the generalization of the AdS/CFT correspondence can realize some more realistic systems, such as QCD-like theories or QCD itself, which have running coupling constants (hence are not conformal), fundamental matter, and reproduce some phase transitions. Recent reviews on the connection between string theory and QCD can be found in [5,6].

New observational results from the relativistic heavy ion collider (RHIC) [7] data tell us that the shear viscosity of the hot plasma is very small [8]; thus the QGP at temperature $T \gtrsim T_{\text{dec}}$ should in fact be strongly coupled [9,10], rather than asymptotic free as we used to think about it,

where T_{dec} is the critical temperature of the confinement/deconfinement phase transition. Hence, all phenomenological applications of QGP, which are based on perturbative QCD or the MIT bag model [11,12], should be reconsidered. These applications include the neutron stars/quark stars and the cosmological QCD phase transition. AdS/CFT provides an excellent tool to study them. Because of its strong interactive nature, it can explore the properties of QGP and the confinement/deconfinement phase transition, in both the high temperature and high baryon number density regions. However, in this paper, we will limit our focus on the property of high temperature region, which is important for the cosmological QCD phase transition.

The organization of this paper is as follows. In Sec. II, we present the results of QGP and the confinement/deconfinement phase transition from AdS/CFT. In Sec. III, we study how these new results affect the conventional scenarios of the cosmological QCD phase transition, including the nucleation rate, the supercooling scale and the mean nucleation distance. We summarize our results in Sec. IV. We will set $\hbar = c = k = 1$ throughout this paper.

II. THE THERMODYNAMICAL AND HYDRODYNAMICAL QUANTITIES OF QGP RECONSIDERED**A. Entropy, free energy, energy, and pressure****1. $\mathcal{N} = 4$ SYM theory**

The gauge fields of large- N_c $\mathcal{N} = 4$ SYM theory are described as open strings ending on N_c Dirichlet 3-branes (D3-branes). In the large 't Hooft coupling limit, $\lambda_4 \gg 1$, the entropy density can be calculated from the Bekenstein-Hawking entropy [13] of nonextremal D3-branes with Ramond-Ramond charge (RR-charge) N_c , which is [14]

$$s = \frac{\pi^2}{2} N_c^2 T^3, \quad (1)$$

where T is identified with the Hawking temperature of the black brane. The result is only 3/4 to that of the free gas case $s_0 = (2\pi^2/3)N_c^2 T^3$. It was argued that the entropy

*congxin.qiu@gmail.com; URL: <http://oxo.lamost.org/>

density can also be calculated from the action I by $Vf = TI = V\epsilon - TVs$ [15], thus $f = -(\pi^2/8)N_c^2 T^4$ [16]. The sound mode dispersion relation of hydrodynamical calculations in the strongly coupled limit gives $c_s^2 = \partial P/\partial \epsilon = 1/3$ and $P + \epsilon = Ts$ [17]; hence, both the energy density ϵ and the pressure P in the strong coupling case, should be only 3/4 to the value of weakly coupled case, which is consistent with the free energy result from the action I . In fact, all CFTs' have similar equation of states (EoS's) up to some numerical factors [18], and what we presented above is just a trivial example.

For the case with not-so-strong coupling, the leading correction is calculated from the action I , which reads [16]

$$s = s_0 \left[\frac{3}{4} + \frac{45}{32} \zeta(3) (2\lambda_4)^{-3/2} + \dots \right], \quad (2)$$

comparing to the weakly coupled case [19,20]

$$s = s_0 \left[1 - \frac{3}{2\pi^2} \lambda_4 + \frac{3 + \sqrt{2}}{\pi^2} \lambda_4^{3/2} + \dots \right]. \quad (3)$$

The 3/4 factor reveals the intrinsic difference between a strongly and weakly coupled system.

2. The QCD-like theories

However, CFTs are very different from QCD in many aspects. For example, (i) their coupling constant λ_4 does not run, hence they experience no conventional phase transitions, and (ii) they can only describes fields in the adjoint (color) but not in fundamental (flavor) representation of the gauge group. The confinement/deconfinement phase transition is always understood as a Hawking-Page phase transition [21] between two background metrics with different free energy density f [15] (except the scenario of [22–24]). The free energy density of the system can be calculated from the volume of spacetime $\int d^D x \sqrt{g}$, and the stable spacetime configuration has the lowest f . Flavors are often added by N_f spacetime filling (flavor) branes [25,26]; however, calculations can be done only in the probe limit (exact quenched approximation), $N_f \ll N_c$. Many efforts have been spent to construct a more QCD-like dual theory. As a phenomenological discussion of their applications to cosmology here in this paper, we do not want to compare their similarity and dissimilarity in detail; however, to make our results more concrete, we do not limit our discussion to some special model. We will reveal the bottom-up way (the AdS-QCD approaches) including the hard-wall [27,28] and soft-wall [29] models, the top-down way including the D3-D7 system [30–33] and the D4-D8- $\bar{D}8$ system (the Sakai-Sugimoto model) [34,35], and also some other phenomenological approaches. The comparative theories include the MIT bag model [11,12], the fuzzy bag model [36], and some lattice results. Most gravity dual theories are limited to the large- N_c limit; however, our QCD has $N_c = 3$, which makes quantitative applica-

tions of the AdS/CFT results difficult. We will try to compare the disagreement between $N_c \rightarrow \infty$ and $N_c = 3$ by some lattice results [37]. Because of the context of this study, we will always assume that the chemical potential $\mu = 0$ in this paper, hence the relation between the free energy density and the pressure is $f = -p$.

Let us first discuss the AdS/QCD approaches. In the hard-wall model, a cutoff is set in the infrared (IR) region to form a slice of AdS₅, which makes the boundary theory confining [27,28]. The two solutions of the Einstein equation are a cutoff thermal AdS and a cutoff AdS with a black hole. For the Ricci flat horizon case [38,39]

$$f_q - f_h = \begin{cases} (\pi^4 L^3 / 2\kappa_5^2) T^4 & T < 2^{-1/4} T_{\text{dec}} \\ -(\pi^4 L^3 / 2\kappa_5^2) (T^4 - T_{\text{dec}}^4) & T > 2^{-1/4} T_{\text{dec}} \end{cases}, \quad (4)$$

where the subscript h indicates the confining phase, q indicates the deconfining phase, $\kappa_5^2 = 8\pi G_5$ describes the gravitational coupling scale, and L is the radius of the AdS space. For the spherical horizon case with sufficient small IR cutoff r_0 , we have [40]

$$f_q - f_h = -\frac{2\pi^2 \Omega_3}{9\kappa_5^2} T_{\text{dec}}^2 \left(r_+^4 - 2r_0^4 - \frac{9r_+^2}{4\pi^2 T_{\text{dec}}^2} \right), \quad (5)$$

where $\Omega_3 = 2\pi^2$ and $r_+ = (3/8\pi T_{\text{dec}}) (\sqrt{9T^2/T_{\text{dec}}^2 - 8} + 3T/T_{\text{dec}})$. The latter case has little physical applications; however, it has thermodynamical properties similar to the soft-wall case.

In the soft-wall model, the IR cutoff is replaced by a smooth cap off, which is realized by the dilaton term in the Einstein action [29]. The difference of the free energy density of the two phases is [38]

$$f_q - f_h = \frac{\pi^4 L^3}{\kappa_5^2} T^4 \left[e^{-x}(x-1) + \frac{1}{2} + x^2 \text{Ei}(-x) \right], \quad (6)$$

where $x = (T_{\text{dec}}/0.491728\pi T)^2$, and $\text{Ei}(-x) = -\int_x^\infty e^{-t}/t dt$.

For a ten-dimensional ‘‘AdS/QCD cousin’’ model with the metric of a deformed AdS₅ black hole crossing some five-dimensional compact space [41], the free energy density is

$$f_q - f_h = -\frac{\hat{s}}{4} T^4 \left\{ \left(1 - \frac{T_{\text{dec}}^2}{T^2} \right) + \left[-\frac{1}{4} \frac{T_{\text{dec}}^4}{T^4} \ln \left(\frac{T_{\text{dec}}^2}{T^2} \right) - 0.039 \frac{T_{\text{dec}}^4}{T^4} + \sum_{n=3}^{\infty} \frac{(-1)^n}{2^{n-1}(2-n)n!} \left(\frac{T_{\text{dec}}^2}{T^2} \right)^n \right] \right\}, \quad (7)$$

which is related to a entropy density $s = \hat{s} T^3 \exp(-T_{\text{dec}}^2/2T^2)$. This model may be applicable to QCD for $1.2T_{\text{dec}} < T < 3T_{\text{dec}}$. It has a good asymptotic behavior $\lim_{T \rightarrow \infty} s \propto T^3$ as a four-dimensional thermal system, because the contributions of the Kaluza-Klein modes

are not taken into account. When $T_{\text{dec}} \ll T$, the result coincides the fuzzy bag model [36] in pure glue case, which restricts $B_{\text{fuzzy}} = f_{\text{pert}} T_{\text{dec}}^2 = (\hat{s}/4) T_{\text{dec}}^2$, $B_{\text{MIT}} = 0$ hence $f_q - f_h = -(\hat{s}/4) T^4 (1 - T_{\text{dec}}^2/T^2)$.

There are also some other models, like the one defined by some complex metric in [42], the one include a non-trivial dilaton flow deformation [43], or the MIT bag model itself. They all have $f_q - f_h \propto T_{\text{dec}}^4 - T^4$, hence are identical with each other up to an overall constant. And in fact, for small supercooling, they are much similar to what in Eq. (4).

Next, we will discuss the top-down scenarios. In the D3-D7 system [30–33], N_c coincident D3-branes form an extremal black brane with near horizon geometry $\text{AdS}_5 \times S^5$, while N_f coincident probe D7-branes fill AdS_5 (hence, they also extend along the radial direction) and wrap some S^3 inside S^5 . When the D7-branes are separated from the D3-branes in S^5 , the chiral symmetry and conformal invariance are broken. When the temperature is low, the separation is large enough that the brane tension can avoid the D7-branes falling into the black brane, hence the branes are ‘‘Minkowski’’ embedded outside the horizon. However, when the temperature is high enough, the gravitational attraction of the black brane renders the D7-branes a ‘‘black hole’’ embedding [44,45]. The critical temperature is T_{fund} , where the mesons melt. The multivalued nature of the free energy density makes the phase transition first order. Nevertheless, for massive fundamental quarks, it is not the temperature of the confinement/deconfinement phase transition, which occurs at some $T_{\text{dec}} < T_{\text{fund}}$. There is as yet a lack of suitable models of confinement/deconfinement phase transition within D3-D7 system. The explicit solutions of $f(T)$, $s(T)$ and $c_s(T)$ are shown numerically in [44,45]. For our purpose, we will not discuss this ‘‘melting’’ transition in detail; notwithstanding, we take notice of some of its critical parameters which can be compared to that in the confinement/deconfinement phase transition. The discontinuity of the entropy density in the phase transition point is

$$\begin{aligned} \Delta s(T = T_{\text{fund}}) &\simeq 0.066 \times \frac{\lambda_4 N_c N_f}{32} T_{\text{fund}}^3 \\ &\simeq 0.032 \frac{T_{\text{fund}}^3}{T^3} \lim_{T \rightarrow \infty} s_{\text{fund}}, \end{aligned} \quad (8)$$

which is proportional to $N_c N_f$, because only the contribution of the fundamental matter is taken into account. The entropy density of massless quarks is $\lim_{T \rightarrow \infty} s_{\text{fund}} = \lambda_4 N_c N_f T^3 / 16$, and the entropy density attributed to gluons is as what in Eq. (1). The superheating and supercooling ranges are (by the system itself rather than by impurities or perturbations)

$$\begin{aligned} \Delta_{<} &= 1 - \frac{T_{\text{min}}}{T_{\text{fund}}} \simeq 0.0019 \quad \text{and} \\ \Delta_{>} &= \frac{T_{\text{max}}}{T_{\text{fund}}} - 1 \simeq 0.0083. \end{aligned} \quad (9)$$

The speed of sound also deviates from $1/\sqrt{3}$ nontrivially when T approaches T_{fund} . However, unless in the extreme supercooling case, c_s would not be vanishing.

Does this melting transition happens in QCD? This is an intractable question. Even if we neglect the influences of the large- N_c and the probe simplifications, we will still need QGP remaining strongly coupled at T_{fund} ; because when it is weakly coupled, the melting of the mesons should be a crossover. As we will see later, the numerical values of Δs , $\Delta_{<}$ and $\Delta_{>}$ are all much smaller than the typical confinement/deconfinement case; besides, we do not really know how to estimate the surface tension σ_{fund} of this phase transition. In addition, melting of different mesons may be asynchronous in QCD. Of course, if it is indeed a phase transition in QCD, it can also affect the evolution of our universe.

In the Sakai-Sugimoto model [34,35], when the temperature is low enough, the N_c coincident D4-branes are compactified on a supersymmetry-breaking spacelike S^1 to make the low energy QCD-like theory (3 + 1)-dimensional, while the N_f D8- $\overline{\text{D8}}$ pairs (with D8 and $\overline{\text{D8}}$ -branes coincide, respectively) cross the S^1 circle at some characteristic points. Gauge bosons are regarded as massless modes of open strings with both ends on D4-branes, while fundamental fermions correspond to open strings with one end in some D4-brane and another end in some D8 or $\overline{\text{D8}}$ -brane. However, when the temperature is high enough [46], to make a lower free energy, the compactified D4-brane direction is not spacelike but in fact timelike. This is the confinement/deconfinement phase transition, because the topological change of the spacetime makes the expectation value of a temporal Wilson loops change from $\langle W(C) \rangle = 0$ to $\langle W(C) \rangle \neq 0$. The spontaneous chiral symmetry breaking is understood as when the N_f D8-branes and N_f $\overline{\text{D8}}$ -branes merge at some radial position u_0 away from the horizon (where we live), which happens at some temperature higher or equal to T_{dec} . The difference between the free energy densities of the two phases can be calculated from the DBI action. This phase transition is first order,

$$f_q - f_h = -\frac{40960\pi^{11}}{729} \frac{l_s(g_s N_c) N_c^2}{T_{\text{dec}}} (T^6 - T_{\text{dec}}^6). \quad (10)$$

For its AdS_6 noncritical string ‘‘cousin’’ model [47], $f_q - f_h \propto -N_c^2 (T^5 - T_{\text{dec}}^5)$. In the Sakai-Sugimoto model, one always have the speed of sound $c_s = 1/\sqrt{5}$ [48]. Because $l_s(g_s N_c) = g_5^2 N_c / (2\pi)^2 = g_4^2 N_c / (2\pi)^3 T_{\text{dec}} = \lambda_4 / (2\pi)^3 T_{\text{dec}}$, and $\lambda_4 N_c / 216\pi^3 \simeq 7.45 \times 10^{-3}$ from meson spectrum [35], we see that the coefficient of Eq. (10) is

really huge. However, these results are quantitatively far from QCD; the unwanted Kaluza-Klein modes of the compactified dimensions cause the theories lacking of the asymptotic UV behavior $f \propto N_c^2 T^4$ while $T \rightarrow \infty$. As we will scale all these theoretical models to QCD by their high temperature behavior, we will not consider the Sakai-Sugimoto model from now on.

There are also some more phenomenological approaches to the EoS's of the QCD-like theories. Gürsoy *et al.* considered a five-dimensional gravity theory coupled to a dilaton field [49,50]. The thermodynamics of this system can be determined uniquely by a positive and monotonic potential $V(\lambda) = 12[1 + \lambda + V_1 \lambda^{2Q} \log^P(1 + V_2 \lambda^2)]$, where $\phi = \log \lambda$ is the dilaton field [51,52]. The theory is confined when $Q = 2/3$ and $P > 0$, or $Q > 2/3$. After chosen some specific potential, the temperature is fixed uniquely by the horizon value of λ , and the EoS can be given by some numerical calculations of the black hole configuration while varying $\lambda(r_H)$. The aim of this model is still limited to explain the finite temperature large- N_c Yang-Mills theory by these authors; however, we may expect that can tell us something more about QCD.

Gubser *et al.* considered another five-dimensional gravity theory coupled to a single scalar [22]. Based on a lot of assumptions, it is shown that the potential of a scalar field $V(\phi)$ and the EoS of the boundary theory have one-to-one correspondence. The results may be applicable for regions both \geq and $\leq T_{\text{dec}}$. Various $V(\phi)$'s correspond to different EoS's, include crossover, first order, and second order phase transitions; hence, the authors expect their model can mimic the EoS of QCD. We choose in this study the potential $V(\phi) = [-12 \cosh(\gamma\phi + b\phi^2)]/L^2$ with $\gamma = \sqrt{7/12}$ and $b = 2$ for the first order case when making comparison with other models [53], but keep γ as a free parameter in the discussion of Sec. III C 2.

The phenomenological model in [49,50] coupled to the dilaton potential $V(\phi)$ has a more solid theoretical foundation; however, the calculation of the EoS's is more complicated than the latter one. As we need to exploit a whole family of EoS's for our astrophysical purpose (especially in Sec. III C 2), we will limit our discussion to the latter model. It should be noteworthy to review the astrophysical application of the first model, especially after some quantitative comparisons between it and the lattice results that have been done.

The comparisons of the free energy density f , the entropy density s , and the square of sound speed c_s^2 for various models, are shown in Fig. 1–3. We scale all thermodynamical quantities by T_{dec} and $\lim_{T \rightarrow \infty} (\bullet)/(\bullet)_{q,\text{SB}} = 3/4$, where ‘‘SB’’ denotes the Stefan-Boltzmann values of thermal quantities in the corresponding QGP phase, except the model discussed in [51,52]. The scaling relation is based on Eq. (1) and the fact that all gravity dual theories are strongly coupled; we assume that all fields considered are UV conformal, and the coefficient 3/4 is universally

applicable for them all. The model in [51,52] is excluded, because it is indeed weakly coupled in the UV region and asymptotically Stefan-Boltzmann. The rescaling is of course reasonable for the entropy s in Fig. 2, because in

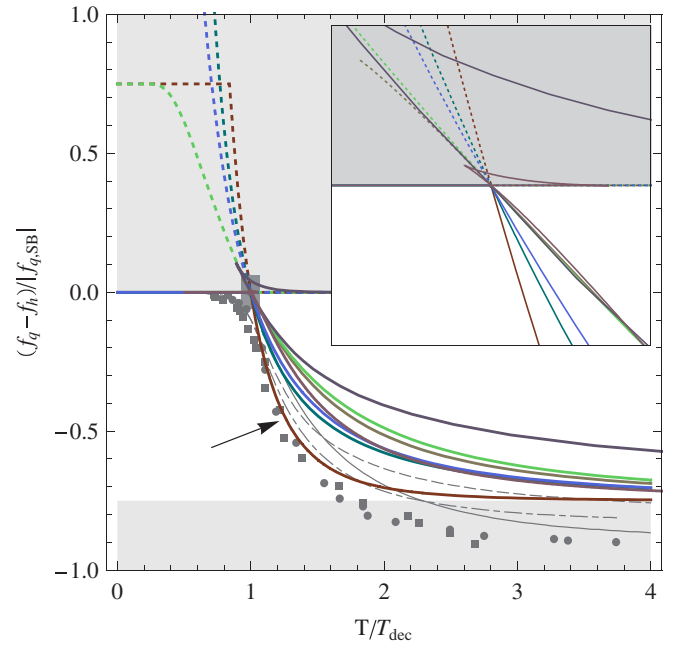


FIG. 1 (color online). The free energy density for various models compares to the free gas case. For the reason that all gravity dual theories are strongly coupled, we scale $(\bullet)/(\bullet)_{q,\text{SB}}$ to 3/4 as $T \rightarrow \infty$, based on the $\mathcal{N} = 4$ SYM result in Eq. (1), where (\bullet) can be replaced by any thermodynamical quantities, such as entropy, free energy, energy, or pressure. The MIT bag model [11,12] and the fuzzy bag model [36] are also scaled to 3/4 by some comparison reasons; they can be easily transform back to their original form if needed. For clarity, we classify and tag our models by numbers. From the arrow direction marked in this figure, the thick lines are for the models (1 \rightarrow 4 \rightarrow 5 \rightarrow 7 \rightarrow 2 \rightarrow 3 \rightarrow 6), respectively. Line (Model) (1) denotes the hard-wall model with the Ricci flat horizon calculated in Eq. (4), models considered in [42,43], and the MIT bag model itself. We neglect their divergent when $T < 2^{-1/4} T_{\text{dec}}$. Line (2) denotes the hard-wall model with the spherical horizon in Eq. (5). Line (3) indicate the soft-wall model case, as Eq. (6) shows. Line (4) indicate the ten-dimensional ‘‘AdS/QCD cousin’’ model in Eq. (7). Line (5) denotes the fuzzy bag model result for comparison with Line (4). Line (6) is for the Gürsoy *et al.* model given in [51]. Line (7) is calculated by the phenomenological model of [22], with a scalar potential $V(\phi) = [-12 \cosh(\sqrt{7/12}\phi + 2\phi^2)]/L^2$. The thin gray lines are the p4-action result [117], in which the solid line indicates the pure glue case, the dashed line for the (2 + 1) flavor case, and the dashed-dotted line for the 3 flavor case. The points are calculated by the lattice methods with almost physical quark masses [118], where small solid bullets for $N_\tau = 4$ case and solid squares for $N_\tau = 6$ case. The small dark region near the critical temperature is enlarged and shown in the top-right corner, where the triangle-like shape formed by some line segments shows clearly the multivalued nature of Line (6) and (7).

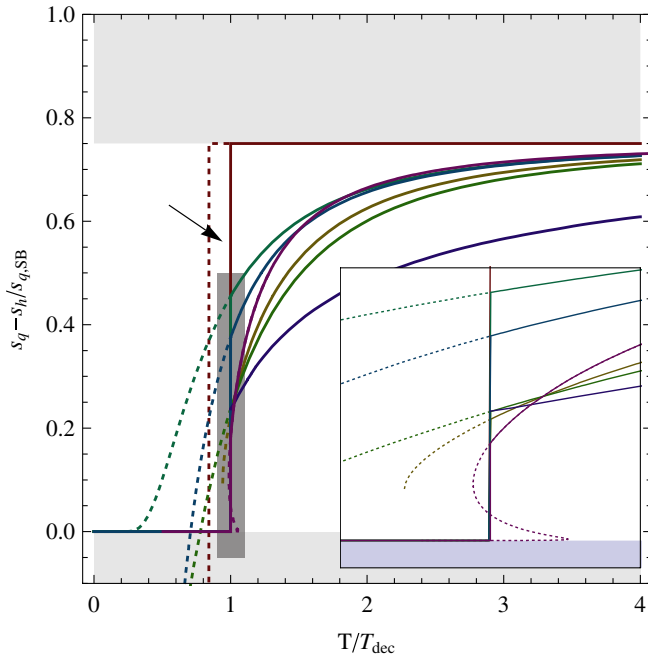


FIG. 2 (color online). The entropy density $s = -df/dT$ for various models compares to the free gas case. In fact, in the large- N_c limit, we have $s_q \propto N_c^2$ and $s_h \propto N_c^0$, hence $s_h = 0$. The notations are as in Fig. 1. The thick lines are models (1 \rightarrow 4 \rightarrow 5 \rightarrow 7 \rightarrow 2 \rightarrow 3 \rightarrow 6), respectively, seeing from the arrow direction.

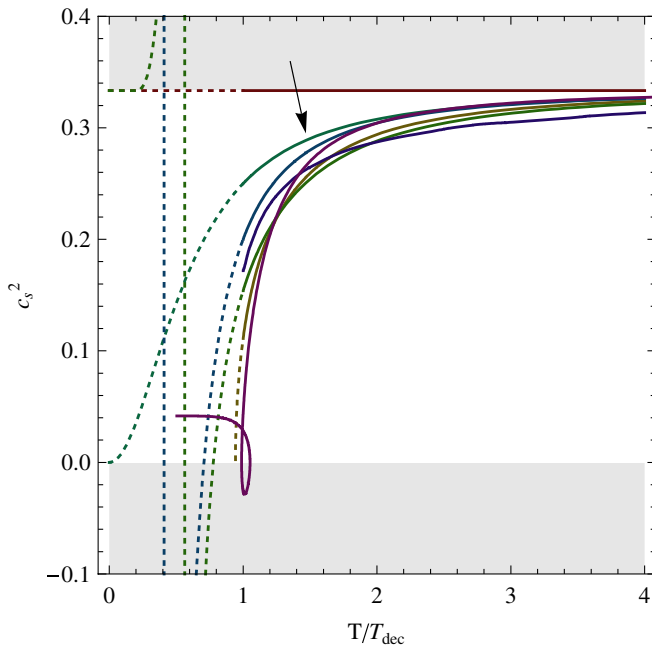


FIG. 3 (color online). The square of sound speed $c_s^2 = d \log T / d \log s$ for various models compares to the free gas case. For the ideal gas case, or the strongly coupled $\mathcal{N} = 4$ SYM theory indicated in Eq. (1), we have $c_s^2 = 1/3$. The notations are as in Fig. 1. The thick lines are models (1 \rightarrow 4 \rightarrow 5 \rightarrow 7 \rightarrow 6 \rightarrow 2 \rightarrow 3), respectively, seeing from the arrow direction.

TABLE I. Comparison of superheating scale $\Delta_> = T_{\max}/T - 1$ and supercooling scale $\Delta_< = 1 - T_{\min}/T_{\text{dec}}$ for various models. The models are numbered as in Fig. 1. The $\Delta_>$ and $\Delta_<$ in the melting transition [44,45] are simply replaced T_{dec} by T_{fund} .

Model No.	$\Delta_>$	$\Delta_<$
1	∞	0.159 (∞)
2	∞	0.057
3	∞	1.
4	∞	1.
5	∞	1.
6	∞	0.111
7	0.046	0.011
melting(T_{fund})	0.0083	0.0019

the large- N_c theories, $s_q \propto N_c^2$ and $s_h \propto N_c^0$; hence the latter one can always be neglected. For the free energy f , things are a little more subtle, since the UV cutoff introduced by the computation [15] do not ensure $f_h \propto N_c^0$. We make the statement as an assumption by using some appropriate counterterms. Although some models (e.g., [22,41]) aim directly at QCD itself, we assume the superheating contributions of f_h and s_h in their models can also be neglected comparing to QGP while $T \rightarrow \infty$. The numbers for the classified models are tagged in Fig. 1. In Table I, we list the maximal superheating and supercooling scale $\Delta_>$ and $\Delta_<$ for various confinement/deconfinement models, and also the melting transition in [44,45]. The existence of $\Delta_>$ and $\Delta_<$ indicates a completely different phase transition process comparing to the old one; for the range of superheating or supercooling is no longer caused by impurities or perturbations, but caused by the theoretical system itself. It can be seen that the melting values are much smaller than the confinement/deconfinement case. In Fig. 4, we compare the latent heat L_h from the theoretical models list above, and from the lattice calculations for various $N_c \geq 3$.

Heuristically, we see that for temperature $2T_{\text{dec}} \leq T \leq 4T_{\text{dec}}$, models (2), (3) and (4), (5), (7) look similar to each other; and for temperature $T \approx T_{\text{dec},+}$, models (2), (3), (6), (7) look similar. Models (2), (3), (6), and (7) have the latent heat a little too small compared to the lattice result of the large- N_c theories, and the latent heat of model (1) and the original MIT bag model seem too large. The discussions of models (6) and (7) may be a little more unreasonable, because the free parameters in the dilaton potential are chosen arbitrarily. The divergence of these models rise because they are all quantitatively far from (large- N_c) QCD. To avoid the unnecessarily complicated details of these models in our discussions in Sec. III, it is worthwhile to ask what kind of feature they have in common. We argue that (i) the EoS of real QCD should be softer than the bag model, and (ii) there exist some intrinsic maximum supercooling scale to be achieved, in contrary to the old belief that the range of supercooling is caused by impurities or perturbations.

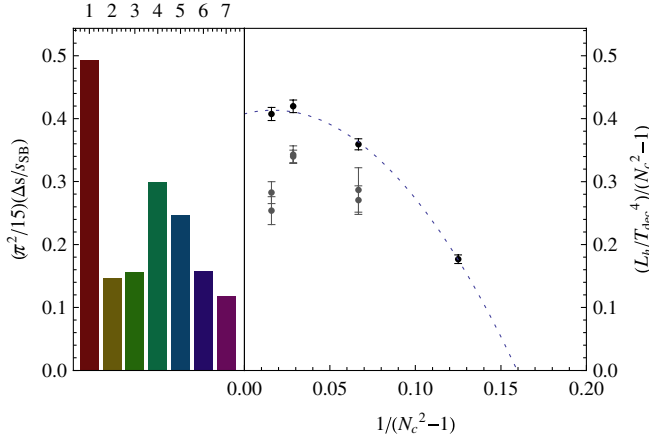


FIG. 4 (color online). The normalization of the latent heat for pure glue fields of various models. In this case, we have $(\pi^2/15)(\Delta s/s_{\text{SB}}) = (L_h/T_{\text{dec}}^4)/(N_c^2 - 1)$. The left part is calculated for various models as tagged in Fig. 1. The right part shows that lattice results for $N_c = 3, 4, 6$, and 8 [37], which suggest that the phase transition is second order for $N_c = 2$, weakly first order for $N_c = 3$, and robustly first order for $N_c \geq 4$. The black error bars are for $L_t = 5$, and the gray ones for $L_t = 6$ and 8 . The fitting line for $L_t = 5$ case is informal, but the extend to $N_c \rightarrow \infty$ case can be guess in this fitting. Notice that the original MIT bag model has the value $\pi^2/15 \approx 0.658$ in this figure.

It is interesting to argue in what conditions the bag-model-like theories can still be applicable. The renormalization-group-improved perturbation expansion method tells us that, when the strong coupling constant α_s increases, the bag constant B_{MIT} decreases [54]. Although this result is only suitable for the perturbative and zero temperature regions, it suggests us to treat the bag model carefully. However, there are indeed a lot of gravity dual theories whose boundary field theories have bag-model-like thermodynamics [38,39,42,43], which do well for explaining meson spectrum or other physical applications.

B. Shear viscosity and bulk viscosity

1. $\mathcal{N} = 4$ SYM theory

The shear viscosity of large- N_c $\mathcal{N} = 4$ SYM theory in the large 't Hooft coupling limit, can be calculated via the Kubo relations. The result is [55,56]

$$\frac{\eta}{s} = \frac{1}{4\pi}. \quad (11)$$

And for bulk viscosity, conformal property requires $\zeta = 0$. It was argued that this value is always available for theories with holographically dual supergravity descriptions [57,58]. For the case of large but finite 't Hooft coupling λ_4 , we have [59,60] $\zeta = \mathcal{O}(\lambda_4^{-3})$ and

$$\frac{\eta}{s} = \frac{1}{4} \left[1 + \frac{135}{8} \zeta(3) (2\lambda_4)^{-3/2} + \dots \right], \quad (12)$$

which can be compared with the weakly coupled case [61]

$$\frac{\eta}{s} \approx \frac{6.174}{\lambda_4^2 \ln(2.36/\sqrt{\lambda_4})}. \quad (13)$$

2. The QCD-like theories

As for the thermodynamical case, people follow the top-down and bottom-up routes to discuss the hydrodynamical quantities of QCD-like theories. However, there is a lack of lattice results to be compared with, because lattice QCD is incapable for real-time behaviors.

To break the conformal behavior of AdS/CFT, one easy way is to consider Dp-branes. The result is [62] $c_s^2 = (5 - p)/(9 - p)$,

$$\frac{\eta}{s} = \frac{1}{4\pi} \quad \text{and} \quad \frac{\zeta}{\eta} = \frac{2(3 - p)}{p(9 - p)}. \quad (14)$$

For the case of compactified Dp-branes, the relations for c_s and η/s are the same as before, but the relation for ζ/η has to be modified to

$$\frac{\zeta}{\eta} = \frac{8d - 2(9 - p)(d - 1)}{d(9 - p)} = 2 \left(\frac{1}{d} - c_s^2 \right), \quad (15)$$

which is consistent with the Sakai-Sugimoto model's result $\zeta/\eta = 4/15$ [48] for $p = 4$ and $d = 3$.

To take into account the contributions of fundamental matter, one can consider the D3-D7 system. The result is [63]

$$\eta = \frac{\pi}{8} N_c^2 T^3 \left[1 + \frac{\lambda_4}{8\pi^2} \frac{N_f}{N_c} h \left(\frac{\lambda_4 T}{M_q} \right) + \dots \right], \quad (16)$$

where M_q is the quark mass, $h(x)$ is some smooth function connects $h(0) = 0$ and $h(\infty) = 1$ by a crossover around $x \sim 1$, with the entropy density $s = (\pi^2/2) N_c^2 T^3 + s_{\text{fund}}$ already been discussed in Sec. II A 2. Similar calculations for the Dp-Dq-D \bar{q} system including the Sakai-Sugimoto model can also be done.

For the models of five-dimensional gravity coupled to some dilaton fields, the bulk viscosity can be calculated directly by the Kubo formula [23,24]. ζ can be estimated by the numerical solution of the metric.

Based on the discussions above and also some other evidences, people conjecture that there may be some universal bounds of shear viscosity $\eta/s \geq 1/4\pi$ (or $\hbar/4\pi k_B$ when getting back the units; also called the Kovtun-Son-Starinets (KSS) bound) for *all physical systems in Nature* [57,58,64], and of bulk viscosity $\zeta/\eta \geq 2(1/p - c_s^2)$ for theories with holographically dual supergravity descriptions [65]. The universality of these bounds suggests that we can use them as critical parameters for the properties of QGP; however, different opinions of them exist in literatures. Clues from the generalization of the second law of

thermodynamics (GSL) suggests some origin of the KSS bound from very basic physical principle [66]; nevertheless, various theoretical models have been constructed which violate the bound, both from quantum field theory [67–70] and from AdS/CFT itself [71,72]. Fortunately, the latter violation only loosens the bound a little, to $\eta/s \geq (16/25)(1/4\pi)$, for the constraint of causality [72,73]. In addition, using the model constructed in [23,24] to calculate the bulk viscosity of the potential $V(\phi) = [-12 \cosh(\gamma\phi + b\phi^2)]/L^2$, can sometimes violate the bound given in [65].

For concreteness, we go back to the case of QGP itself. Let us first discuss the shear viscosity η . Although some theoretical arguments suggest us that η/s should be much larger (maybe by a constant of ~ 7) than $1/4\pi$ in the strong 't Hooft coupling limit, because it is much larger than the $\mathcal{N} = 4$ SYM theory case in the weak coupling limit [61], RHIC results tell us that the η/s of QGP nearly saturates [8,74,75], or maybe even violates [75] the KSS bound.

There are few discussions about the dependence of parameter η on the temperature T . It has been done in the hard-wall and the “AdS/QCD cousin” models [76]; nevertheless, they both always have $\eta/s < 1/4\pi$, which violate the KSS bound. Naïvely, one can estimate it by some phenomenological relation

$$\eta \sim \epsilon l c_s, \quad (17)$$

where l is the correlation length; however, it is very hard to make quantitative computations by this formula. Some interpolation between strong and weak coupling regions may be also possible [77], as the perturbative QCD result of η in the weak coupling region is rather credible [78].

For the case of the bulk viscosity ζ , lattice results of gluodynamics show that it rises sharply when $T \rightarrow (T_{\text{dec}})_+$ [79–81], which are qualitatively consistent with the fact that c_s drops there. Although ζ cannot be calculated in the supercooling region $T < T_{\text{dec}}$ within the lattice framework, we assume from AdS/CFT that it varies smoothly while cross the phase transition point.

C. Surface tension

Very few works exist addressing the surface tension of the confinement/deconfinement phase transition from the AdS/CFT viewpoint. For this purpose, two separate metrics with different topologies, both have $(3+1)$ -dimensional translational invariance within “our world” (as assumed by all the models in Sec. II A 2), are not suitable; as we need nontrivial metric change along the direction of “our world”. Some relative discussions can be found in [82]. Deconfined regions map to some pancake-like black hole solutions, whose interior resembles black brane; however, they have domain-wall-like boundary to smoothly connect with the confined gravity solution. Hence, the hadronization of the plasma balls can be understood as the Hawking radiation of the dual black holes.

Although this work aims particularly at the large- N_c gauge theories, some other authors believe that dual black holes are in fact produced inside of RHIC [83,84].

The concrete calculation is based on some finite temperature Scherk-Schwarz compactification metrics, which have covering space asymptotically AdS_{d+2} near the boundary. Both the time direction τ and a spacelike direction θ are compactified to some circles S^1 ; however, the θ circle shrinks to zero at some finite $u = u_0$ in the confined phase, rather than the τ circle shrinks to zero in the deconfined phase. The metric of the domain-wall-like boundary can be solved numerically, and the surface tension can be estimated by it. The surface tension σ is rounded to numbers $2.0\epsilon_q(T_{\text{dec}})/T_{\text{dec}}$ for $d = 3$ (a hence $(2+1)$ -dimensional gauge theory) and $1.7\epsilon_q(T_{\text{dec}})/T_{\text{dec}}$ for $d = 4$ (a hence $(3+1)$ -dimensional gauge theory). $\sigma \propto \epsilon_q \propto N_c^2$ is a natural result of the scaling of the classical gravity action. The aftermath of this fact is discussed in Sec. III C 1.

However, there are some relevant discussions of the surface tension σ , based on both lattice gauge theory and the MIT bag model. The lattice results of σ for the pure gluon $SU(3)$ gauge theory are around $0.02T_{\text{dec}}^3$ [37,85,86]. In the MIT bag model, the contribution of σ is divided to an intrinsic and a dynamical surface tension [54]. The intrinsic surface tension σ_I is suggested to be very small; however, we do not know how to calculate it in this framework. The dynamical surface tension σ_D raises from the modification of the fermion density in the phase transition surface; hence, it depends sensitively on the strange quark mass. Detailed calculation shows that σ_D is at most $(60 \text{ MeV})^3$ [87]. Notice that the bag model results are only valid for the zero temperature case, and the lattice results do not consider fundamental quarks (which is supposed to be crucial in the bag model discussions). However, these results may suggest that σ is not very large.

III. THE COSMOLOGICAL QCD PHASE TRANSITION RECONSIDERED

If the QCD confinement/deconfinement phase transition is first order, just as what the application of a Hawking-Page phase transition indicates, our universe underwent that transition when it was about 10^{-5} s old. Generically, if the surface tension of the transition interface is nonzero, the universe should be supercooled for some scale before nucleation indeed happens [88,89]. After the supercooling stage, some hadronic bubbles are created; they may then expand rapidly as both the detonation [90–92] and deflagration [91–93] waves. For the deflagration wave case, the latent heat released by the phase transition, reheats our universe back to T_{dec} . After that, the phase transition goes along synchronously while the universe expands, and converts the denser QGP matter to the less-dense hadronic matter mildly. The mean distance between the hadronic bubbles, is calculated in [94–98]. After about half of the

QGP matter has been converted, the hadronic bubbles are replaced by the QGP bubbles. As the phase transition goes on, the QGP bubbles disappear more and more rapidly [99]. Baryons may be concentrated in the QGP bubble, and relics such as quark nuggets may be produced [100]. Some panoramic description of this phase transition can be found in [101], and some up to date review articles are in [1,2].

The process we described above is called *homogeneous nucleation*. We will not consider other possibilities such as heterogeneous nucleation [95,98] or inhomogeneous nucleation [102] in this paper, because they are less sensitive to the intrinsic properties of QCD (hence, less sensitive to the AdS/CFT results) than the homogeneous case. In addition, we will not consider the late stage issues of this phase transition, such as the stability of quark nuggets, because the zero chemical potential assumption is no longer suitable there. We leave the relative discussions in the follow-up studies, by which the results from the finite chemical potential AdS/CFT correspondence can be used directly.

A. The nucleation rate

The nucleation rate of the hadronic phase out of the QGP phase can be calculated as in [103]

$$\Gamma = \frac{\kappa}{2\pi} \Omega_0 e^{-\Delta F(R_*)/T}, \quad (18)$$

where

$$\kappa = \frac{4\sigma(\zeta_q + 4\eta_q/3)}{T^2(s_q - s_h)^2 R_*^3} \quad (19)$$

is the dynamical prefactor to describe the dissipation effect,

$$\Omega_0 = \frac{2}{3\sqrt{3}} \left(\frac{\sigma}{T}\right)^{3/2} \left(\frac{R_*}{\xi_q}\right)^4 \quad (20)$$

is the statistical prefactor, and

$$\Delta F(R_*) = \frac{16\pi}{3} \frac{\sigma^3}{(f_q - f_h)^2} \quad (21)$$

is the additional free energy of a hadronic bubble of the critical size $R_* = 2\sigma/(f_q - f_h)$ within the QGP phase, ξ_q is the correlation length in the QGP phase. For the case of zero chemical potential, we have $f_q - f_h = P_h - P_q$ and the enthalpy density $\omega = sT$.

The prefactor $(\kappa/2\pi)\Omega_0$ in the nucleation rate formula for various models, is shown in Fig. 5. The most important step is how to map the various thermodynamical quantities of large- N_c theories from AdS/CFT models to real QCD. Our strategy is linearly map $(\bullet)_{q,SB}$ to the corresponding quantities of the $g_q = 37 + 14.25$ ideal gas model, and map the $f_q = f_h$ and $s_q = s_h$ horizontal lines in Fig. 1 and 2 to the $g_h = 3 + 14.25$ ideal gas model, where g_q and g_h are the degrees of freedom of the real world at $T = T_{dec} \approx$

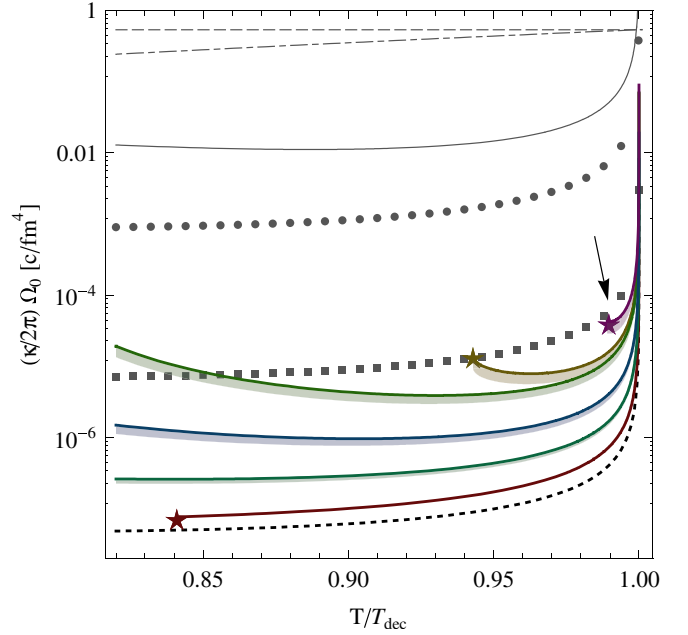


FIG. 5 (color online). The prefactor $(\kappa/2\pi)\Omega_0$ in the nucleation rate formula. The thin gray dashed and dashed-dotted lines on the top are for dimensional values T_c^4 and T^4 respectively. The thin gray solid line using the same parameters as in [103], is shown for comparison reasons. Its value seems much larger than all other cases, *mainly* because it uses a rather large $\sigma = 50$ MeV/fm² (although other parameters also affect the curve); however, we choose a rather small value of $\sigma = 0.02T_{dec}^3 \approx 3.64$ MeV/fm² for $T_{dec} = 192$ MeV [104] in all other estimations. The gray solid bullet and square lines are for the pure gluon $SU(3)$ lattice result $L_h = 1.4T_{dec}^4$ and $\sigma = 0.02T_{dec}^3$ [37]. Nevertheless, when calculating the effectively massless degrees of freedom, we also count the fermionic contributions. The difference is the former case uses the perturbative result $\eta_q \approx 1.12T^3/\alpha_s^2 \log(1/\alpha_s)$ and $\alpha_s \sim 0.23$, but the latter case uses the AdS/CFT result $\eta_q = s_q/4\pi$. The thick color lines are for models discussed above. Seeing from the arrow direction, they are models (7 \rightarrow 2 \rightarrow 3 \rightarrow 5 \rightarrow 4 \rightarrow 1), respectively. The process of scaling those large- N_c theories to real QCD, and the rationality of that scaling, are discussed in the main text. The shear viscosity of models (1) and (4) are evaluated by [76]; while for all other cases, we choose $\eta_q = s_q/4\pi$. The bulk viscosities are chosen by the relation $\zeta_q/\eta_q = 2(1/3 - c_s^2)$ of Eq. (15), and the shadow regions show the differences between them and the $\zeta_q = 0$ cases. ζ_q of model (7) can be calculated from more sophisticated numerical results given by [23,24] if needed; however, we deal with it similarly with others for simplification. The black dotted line near the bottom is for the original MIT bag model with $\eta_q = (s_q - s_h)/4\pi$. We choose the correlation length $\xi_q = 0.48(T_{dec}/T)$ fm [119] from lattice result for all our estimations, except the thin gray solid comparison line; in the gravity side, a lower limit of ξ_q is given by [66].

192 MeV [104] before and after the confinement/deconfinement phase transition. The coefficient 14.25, contributed by the leptons and photons, is almost irrelevant to our follow-up discussions, beside the ones using the

Friedmann equations to describe the expanding universe; hence, we will not discuss its rationality. However, the contribution 3 from the pions, actually needs to be studied more carefully. Pionic freedom is caused by the fundamental quarks, while 21 of 37 in g_q is caused by the fundamental quarks as well. As nearly all our models of EoS's are dominated by gluodynamics, and the contribution to the latent heat L_h or the surface tension σ by gluons and quarks cannot be discussed separately, this manipulation is in fact untenable. However, the quenched lattice method faces the same problem. Nevertheless, we take the whole EoS's to describe the thermal quantities in different temperatures, rather than some characteristic parameters like L_h or σ . For some models with free parameters like in [22–24] (which we will discuss especially in Sec. III C 2), we may expect that suitable choice of parameters can absorb the contribution of fundamental quarks. Hence, we expect the calculations below can still reveal some aspects of real QCD.

As seen from Fig. 5, the strongly coupled nature of QGP can lower the prefactor $(\kappa/2\pi)\Omega_0$ a lot, mainly by the reason that it has a relatively smaller shear viscosity $\eta_q = s_q/4\pi$. It is artificial that the lattice results seems much larger than what is in all of our models tagged by numbers. The reason is that, the value $L_h = 1.4T_{\text{dec}}^4$ is calculated by gluodynamics, but it has been shared naïvely to both gauge and fundamental particles by our simple mapping. As the lattice results indicate, the latent heat of QCD with physical quarks may be smaller than pure gauge case, the prefactor may be enhanced. The increasing of $(\kappa/2\pi)\Omega_0$ for some not-very-small supercooling for our models is very interesting. Beside the reason we erase all the reductions for small supercooling, the main reason is when the EoS is not bag-model-like, the latent heat is not as large as in T_{dec} while the supercooling is large. This can be seen roughly from Fig. 2 and the relation $L_h = (4/3)T(s_q - s_h)$.

B. The supercooling scale and the mean nucleation distance

To estimate the supercooling scale quantitatively, we have some separate criteria. If the supercooling is required to complete the phase transition, we need at least one nucleating bubble per Hubble volume; that is, $\Gamma > 1/d_H^3 \Delta t$ for the Hubble radius $d_H = a/\dot{a} = \sqrt{45/4\pi^3} M_{\text{pl}} \cdot g_q^{-1/2} T^{-2}$ and the nucleating duration Δt . We may relax Δt to the Hubble time $d_H/2$, because the resulting supercooling scale is in fact insensitive to this parameter. Hence, the supercooling scale can be roughly estimated by $\Gamma \approx 1/d_H^4$.

To estimate the supercooling scale more accurately, let us consider the deflagration bubble scenario. The applicable parameter space of this scenario is discussed in [92]. Assuming that a hadronic bubble created in the supercooling QGP phase expands deflagratingly, a shock wave with

velocity $v_{\text{sh}} \gtrsim c_s$ preheats the QGP matter to stop the new nucleating processes there, and a deflagration wave with relatively slow velocity v_{def} burns the QGP matter to hadronic matter behind it [91–93]. The velocities v_{sh} and v_{def} are calculated accurately in [92]. The weakly and electromagnetically interacting particles can affect these velocities [105,106]; however, deflagration happens only during the early stages for the small supercooling case, when their influences are negligible. When most of the space has been swept by the shock wave, the supercooling process ceases. The fraction of space which has already been swept by the shock wave is calculated foremost in [107,108]. For our purpose, we can neglect the expanding of the universe in the supercooling timescale. Hence, the criterion of the supercooling scale T_f is roughly [89]

$$\frac{4\pi}{3} \int_{t_{\text{dec}}}^{t_f} \Gamma v_{\text{sh}}^3 (t_f - t)^3 dt \approx 1, \quad (22)$$

where $t_{\text{dec}}(T_f)$ is the age of the universe at temperature $T_{\text{dec}}(T_f)$. This integral equation can be solved approximately by

$$\left[-\frac{\sqrt{24\pi G} \cdot \epsilon_q^{1/2} (p_q + \epsilon_q)}{d\epsilon_q/dT} \frac{d(\Delta F/T)}{dT} \right]^4 \approx 8\pi \left(\frac{\kappa}{2\pi} \Omega_0 \right) v_{\text{sh}}^3 e^{-\Delta F/T} \Big|_{T_f}, \quad (23)$$

in which we deal with the Friedmann equations without any assumption about the EoS of the QGP phase.

The numerical result of $\Delta = 1 - T_f/T_{\text{dec}}$ depends on various surface tension σ for various models, is shown in Fig. 6. For small σ , the system follows nicely to the relation $\Delta \propto \sigma^{3/2}/L_h$ [95] for fixed L_h ; however, when σ is large enough, these lines tilt up. One reason for these departures from $\sigma^{3/2}$ can be seen from the reduction of Eq. (23) for some EoS's with constant L_h , which gives $\Delta \propto \sigma^{3/2}/\sqrt{171 - 4 \ln(\beta/\sigma^{3/2})}$ for some explicitly written positive β [89]. The other reason is the effective latent heat L_h released drops for some not-very-small supercooling scale for the more realistic EoS's. Nevertheless, comparing to the tilting up of d_{nuc} seen from Fig. 7, the effects here for Δ is really weak. Lines in that figure cannot be extended to larger Δ , in where $d(\Delta F/T)/dT \rightarrow 0$ and our approximation becomes inapplicable. In addition, Δ is totally insensitive to the prefactor in the right hand side of Eq. (23), such as the shear viscosity η_q or the shock viscosity v_{sh} .

In a more accurate (and also more sophisticated) way, supercooling scale can be calculated dynamically from the time evolution of the temperature [109]. We do not calculate the time-dependent solutions here, because our qualitative QCD theories still have too many free parameters, thus intrinsic discussions are not very easy. Nevertheless,

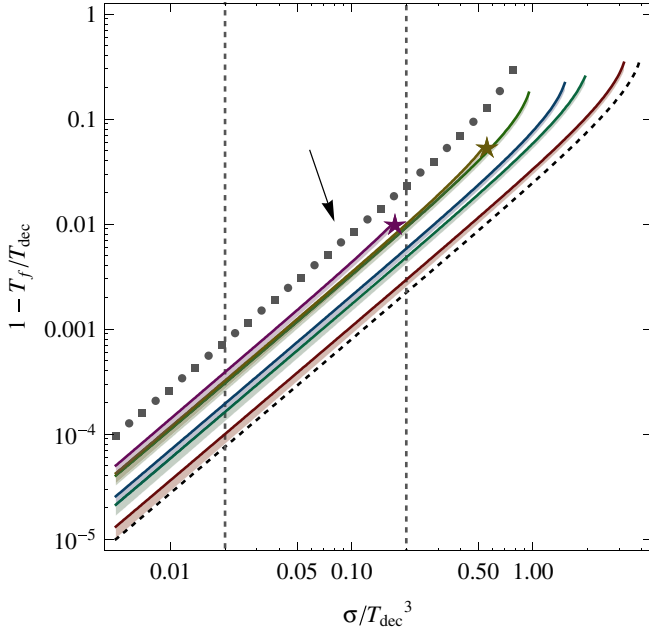


FIG. 6 (color online). The supercooling scale $\Delta = 1 - T_f/T_{\text{dec}}$ depends on the surface tension σ for various models, which is estimated by Eq. (23). The notations are as in Fig. 5, except the shadow regions around the lines show the difference between Eq. (23) and the rough criterion $\Gamma \approx 1/d_H^4$. The two gray vertical dashed lines are marked for $\sigma = 0.02T_{\text{dec}}^3$ and $\sigma = 0.2T_{\text{dec}}^3$, which are chosen as typical parameters in Fig. 9 and 10. It can be seen that the supercooling scale Δ is really insensitive to the method we estimate it, even in the small σ regions where $d_{\text{nuc}} \ll d_H$. The thick lines are models (7 \rightarrow 2 \rightarrow 3 \rightarrow 5 \rightarrow 4 \rightarrow 1), respectively, seeing from the arrow direction. Although v_{sh} can be calculated accurately by [89], we choose $v_{\text{sh}} = c_s$ for simplification, where the differences between them are imperceptible.

we think that there should be some interesting results in the not-very-small supercooling regions.

The mean nucleation distance of the hadronic bubbles in the phase transition era, can be estimated by $d_{\text{nuc}} \approx n(t_f)^{-1/3}$ and the bubble number density calculated in [107,108]. Some suitable reductions give $d_{\text{nuc}} \approx (8\pi)^{1/3} v_{\text{sh}} / (-d(\Delta F/T)/dt|_{t_f})$ [97]. Considering some special EoS, we have

$$d_{\text{nuc}} \approx \frac{(8\pi)^{1/3} v_{\text{sh}}}{\sqrt{24\pi G}} \frac{d\epsilon_q/dT}{\epsilon_q^{1/2}(p_q + \epsilon_q)} \frac{dT}{d(\Delta F/T)} \Big|_{T_f}. \quad (24)$$

The numerical result of d_{nuc} is shown in Fig. 7. It can be seen that for small σ , $d_{\text{nuc}} \propto \sigma^{3/2}/L_h$ for fixed L_h , as is estimated in [95,98]; however, when σ becomes large, d_{nuc} tilts up caused by both a more accurate treatment of supercooling and the drop of L_h for some more realistic EoS's. Although models (2) and (7) both have some maximum σ where $\Delta_{<}$ is saturated, their behavior are completely different. In model (2), $L_h \rightarrow 0$ hence $d_{\text{nuc}} \rightarrow \infty$

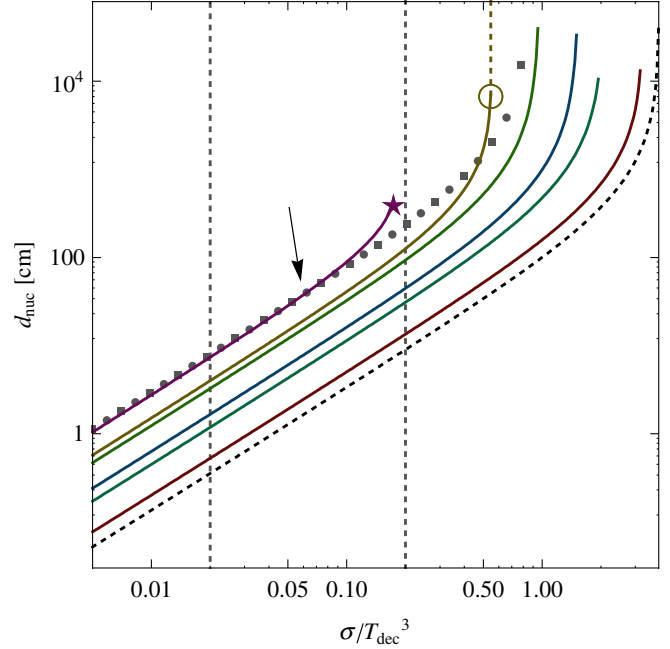


FIG. 7 (color online). The mean nucleation distance d_{nuc} depends on various surface tension σ , estimated by Eq. (24). The notations are as in Fig. 5. The thick lines are models (7 \rightarrow 2 \rightarrow 3 \rightarrow 5 \rightarrow 4 \rightarrow 1), respectively, seeing from the arrow direction. Although the terminal point “ \star ” marked for model (7) is factual, the terminal point “ \circ ” marked for model (2) is the numerical limit of our calculation. A maximum σ exists for the maximum expected supercooling scale to be achieved; as $L_h = 0$ for $\Delta = \Delta_{<}$ in model (2), $d_{\text{nuc}} \rightarrow \infty$ when σ tending towards this limit.

while $\Delta \rightarrow \Delta_{<}$; but in model (7), $L_h \neq 0$ hence d_{nuc} is finite.

C. The supercooling scale and the mean nucleation distance once more

It may not be plausible to consider the dependence of the supercooling scale Δ and the mean nucleation distance d_{nuc} on the surface tension σ . New phenomena deviating from the rough analytic estimations $\Delta \propto \sigma^{3/2}/L_h$ and $d_{\text{nuc}} \propto \sigma^{3/2}/L_h$ [95], always appear in the regions where σ is large enough. Although σ is indeed a free parameter since we do not know its value, it should not be very large both from the lattice results of gluodynamics [37,85,86] and some theoretical estimations based on the MIT bag model [54,87]. This issue has already been discussed in Sec. II C.

Notwithstanding, we can still do some qualitative or quantitative estimations, and give some constraints on both the surface tension σ and the latent heat L_h .

1. The global constraint of the surface tension on the large- N_c theories

In [37], the authors argued one cannot distinguish the scaling of the surface tension $\sigma \propto N_c$ or $\sigma \propto N_c^2$ from their

lattice analyses of $SU(N_c)$ gauge theories. However, for the reason that we definitely know the latent heat $L_h \propto N_c^2$ for a first order phase transition, if this transition indeed exists, to avoid a zero nucleation rate in Eq. (18), we need at most $\sigma \propto N_c^{4/3}$.

If in some large- N_c theories, σ depends on N_c sharper than $N_c^{4/3}$, we can equivalently give an upper limit for N_c . For the finite temperature Scherk-Schwarz compactification model, the domain wall tension $\sigma \propto \epsilon_q/T_{\text{dec}} \propto N_c^2$ has been calculated numerically [82] for the compactified AdS_5 and AdS_6 soliton solutions. Hence, given an explicit expanding universe, we can restrict N_c by the phase transition happened there. A special example to constrain N_c of the large- N_c CFT in the holographic Randall-Sundrum (RS) I model, is given in [110,111], despite of the fact that the concept of the surface tension does not intervene their discussions. The exponential suppressive factor in the nucleation rate formula, is given by the Euclidean action which has a minimum at $T = 1/\sqrt{3}T_c$ for some transition happens at T_c . The comparison between the holographic RS I phase transition and our model based on AdS/CFT, is given in Sec. IV.

2. The extremely weakly first order confinement/deconfinement phase transition?

The order of the confinement/deconfinement phase transition for QCD with physical quark masses, is still being debated. The lattice results of quenched QCD suggest that it is at most weakly first order [86]. However, adding massive quarks seems to make the transition weaker, or even gradually changing it to a rapid crossover [112,113]. Hence, one possibility to be considered is the extremely weakly first order case. We still assume the bubbles expand deflagrantly in this case.

Naïvely, both the supercooling scale Δ and the mean nucleation distance d_{nuc} increase reciprocally while the latent heat L_h decreases, base on the rough analytic estimations $\Delta \propto \sigma^{3/2}/L_h$ and $d_{\text{nuc}} \propto \sigma^{3/2}/L_h$ [95]. However,

more abundant phenomena can happen for more realistic EoS's of QCD.

These phenomena are caused mainly by two reasons. (i) If the EoS's possesses the weakly first order phase transitions, the effective L_h decreases when the supercooling scale becomes large. This can easily be seen from Fig. 2 and the relation $L_h = (4/3)T(s_q - s_h)$. (ii) As a universal property of the Hawking-Page phase transition [21], there is a minimum temperature $T_{\text{min}} < T_{\text{dec}}$ below which the high temperature phase cannot exist. It is illustrated in Fig. 8. The qualitative effect of the first reason has already been discussed in [97]. We will give here both quantitative effects of (i) for some specific EoS's, and also some qualitative effects of (ii).

For our discussions, we will use the mimicking model of Gubser *et al.* [22–24]. The reason is that, it is convenient to use its potential $V(\phi)$ to construct a first order phase transition with decreasing L_h , which then transforms smoothly to a rapid crossover. Another phenomenological model including a dilaton field given in [51,52] may also be used, as it has a more solid theoretical foundation. We omit the discussions of it here, because the work for this model itself is still on its way, and the calculation of the EoS's is more complicated than the former one. Some qualitative properties, such as $\Delta_<$ decreases with decreasing L_h , are supposed to be universal.

As the potential of the Gubser *et al.* model $V(\phi) = [-12 \cosh(\gamma\phi) + b\phi^2]/L^2$ has two parameters γ and b , in fact, our method applies to a wide range of models (potentials) with one free parameter. We fix $b = 2$ and evaluate $\gamma \in [0.722, 0.790]$ (formerly we used $\gamma = \sqrt{7/12} \approx 0.764$); when doing this, the latent heat L_h varies from 0.69 to $3.77T_{\text{dec}}^4$. The dependence of d_{nuc} and the supercooling scale Δ on L_h are shown in Fig. 9 and 10. Observing from the figures, when L_h is large enough, it follows the scaling law $\Delta \propto L_h^{-1}$ and $d_{\text{nuc}} \propto L_h^{-1}$; however, for smaller L_h , d_{nuc} tilts up because the effective L_h drops for reason (i). In a large acceptable parameter space, d_{nuc} is not as small as people used to think as about ≈ 2 cm [98]

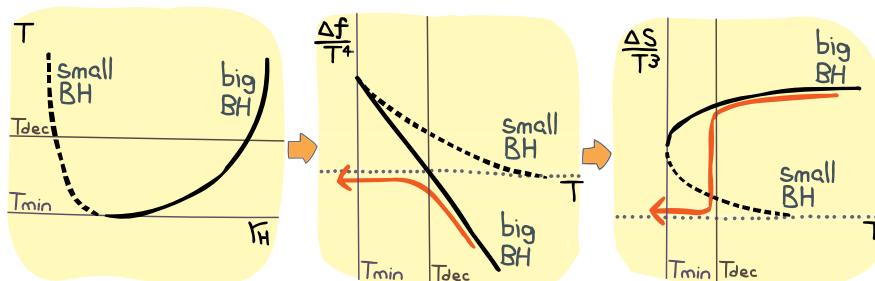


FIG. 8 (color online). A Hawking-Page phase transition [21] should always have a minimum temperature T_{min} , below which the high temperature phase cannot exist. This minimum temperature is intrinsic, rather than caused by impurities or perturbations in the old supercooling scenarios. The long curved arrows show the behavior of the system from high temperature to low temperature phase, if no supercooling happens.

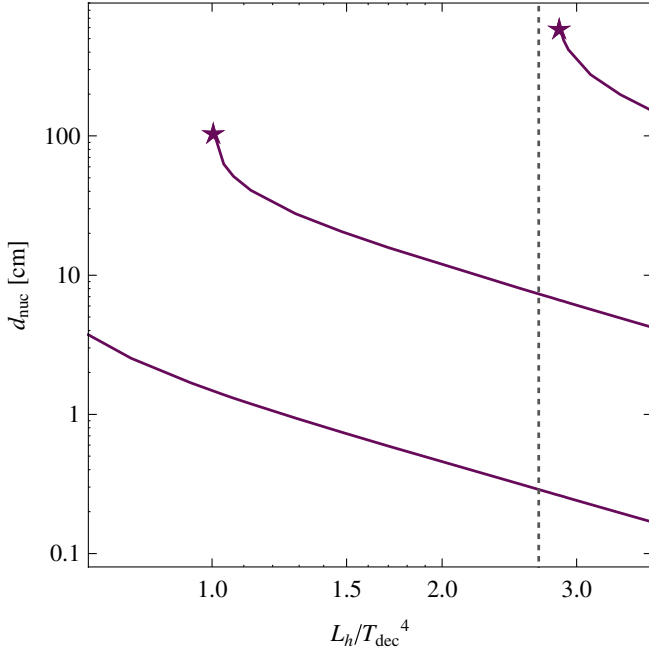


FIG. 9 (color online). The mean nucleation distance d_{nuc} depends on the latent heat L_h for the Gubser *et al.* model [22]. The gray vertical dashed line is $L_h = 2.67T_{\text{dec}}^4$ deduced from the potential $V(\phi) = [-12 \cosh(\sqrt{7/12}\phi) + 2\phi^2]/L^2$ in the formal estimations. The three thick lines are for $\sigma = 0.2T_{\text{dec}}^3$, $0.02T_{\text{dec}}^3$ and $0.002T_{\text{dec}}^3$ (from up to down), respectively.

for the homogeneous nucleation case. For some definite σ , there exist some minimum $L_{h,<}$, where the maximum supercooling $\Delta_{<}$ is achieved.

What happens if the realistic L_h is smaller than $L_{h,<}(\sigma)$? Maybe this situation never happens in a consistent world. In despite of that, as a lack of the complete origin of the surface tension, we just treat L_h and σ as free parameters. If this happens, we have the bubble number density

$$n(t_{<}) \simeq \left(\frac{\kappa}{2\pi} \Omega_0 \right) \frac{e^{-\Delta F/T}}{-d(\Delta F/T)/dt} \Big|_{t=t_{<}} \ll \frac{[-d(\Delta F/T)/dt]^3}{8\pi v_{\text{sh}}^3} \Big|_{t=t_{<}}, \quad (25)$$

comparing with Eq. (24) and the discussions in [97], where $t_{<}$ is the time when the minimum temperature $(1 - \Delta_{<})T_{\text{dec}}$ is achieved. Because of the exponential suppressed factor $\exp(-\Delta F/T)$, this situation will lead to a much smaller bubble number density n hence a much larger d_{nuc} . One may think that the larger d_{nuc} can help surviving the quark nuggets, or provide the inhomogeneous initial conditions of the big-bang nucleosynthesis (BBN). However, this scenario is in fact rather hard to appear. We also show in Fig. 10 the criterion $\Gamma \simeq 1/d_H^4$, that is, the supercooling scale needed for $d_{\text{nuc}} \simeq d_H$. Because d_{nuc} varies too sensitively to the supercooling

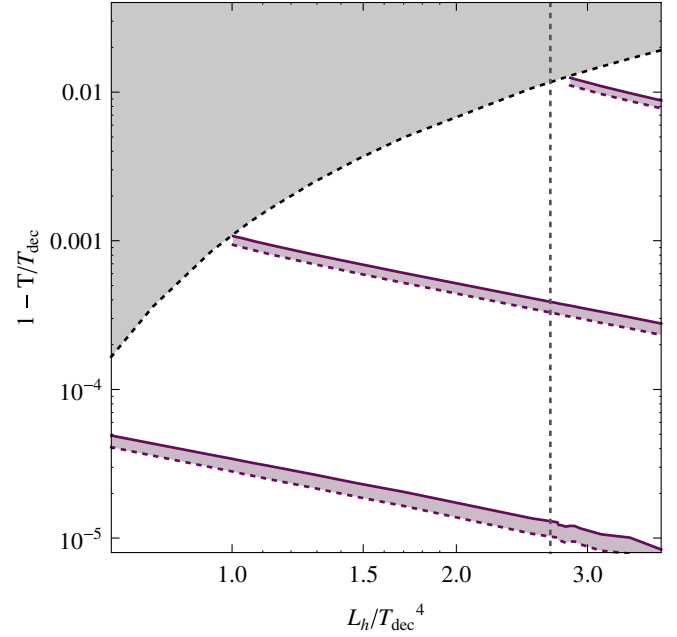


FIG. 10 (color online). The various supercooling scales depend on the latent heat L_h for the Gubser *et al.* model [22]. The black dotted curve from the top-right corner to the bottom-left corner is the maximum supercooling scale $\Delta_{<}$; hence the shadow region above it, is forbidden by that model. The actual supercooling scales $\Delta = 1 - T_f/T_{\text{dec}}$ calculated by Eq. (24) are denoted by the thick solid lines, which are for $\sigma = 0.2T_{\text{dec}}^3$, $0.02T_{\text{dec}}^3$ and $0.002T_{\text{dec}}^3$ (from up to down), respectively. The dotted lines a little below them constrain the phase transition to be completed, which are roughly calculated by $\Gamma \simeq 1/d_H^4$; that is, $d_{\text{nuc}} \simeq d_H$. For some particular σ , d_{nuc} can easily be much larger, providing that the latent heat L_h is small enough that the maximum supercooling $\Delta_{<}$ is saturated. However, it is unlikely that the larger d_{nuc} can help us understanding the formation of quark nuggets or the inhomogeneous initial conditions of the big-bang nucleosynthesis, because the parameter L_h should be fine-tuned.

scale, the corresponding L_h has some value very close to $L_{h,<}$. Hence, to get an appropriate d_{nuc} for our universe, we need to fine-tune L_h in a very small region a little smaller than $L_{h,<}$, which is unlikely to be so.

IV. DISCUSSION AND CONCLUSION

In this paper, we discussed some implication of the new AdS/CFT results to the cosmological QCD confinement/deconfinement phase transition. We limit our discussion to the homogeneous nucleation case. The values of the hydrodynamical quantities, like the shear viscosity η or the bulk viscosity ζ , can significantly lower the prefactor $(\kappa/2\pi)\Omega_0$ of the nucleation rate formula compared to the old estimations; however, they can hardly affect other characteristic parameters of this process, such as the supercooling scale $\Delta = 1 - T_f/T_{\text{dec}}$ or the main nucleation distance d_{nuc} . The new EoS's, which differ from the MIT bag model, can

affect the phase transition scenario mainly in two ways. (i) As most of these EoS's are comparatively more weakly first order than the bag model, it is not adequate to treat their latent heat L_h as a constant. For some not-very-small supercooling, the effective latent heat is always much smaller. Hence, d_{nuc} enhances comparing to the old estimation $d_{\text{nuc}} \propto \sigma^{3/2}/L_h$ [95] when σ becomes larger or L_h becomes smaller. In a large acceptable parameter space of σ and L_h , d_{nuc} is not as small as people used to think as about ≈ 2 cm [98] for the homogeneous nucleation case. (ii) The high temperature phase should have an intrinsic maximum supercooling scale $\Delta_<$ based on a Hawking-Page type phase transition. This is in contrast with the old belief that the range of supercooling is caused by impurities or perturbations. We discussed the possibility that this maximum supercooling scale is saturated in the cosmological QCD phase transition, which may happen when this phase transition is extremely weakly first order. If it happens, the nucleation distance d_{nuc} can be increased tremendously. However, it is unlikely to be so; because to get an appropriate d_{nuc} for our universe (that is, to help understand the surviving of the quark nuggets, or to get the appropriate initial conditions of the BBN), L_h needs to be fine-tuned.

Some related works are listed as below for comparison reasons. The nucleation rate and also some of its cosmological applications, base on the holographic RS I model, are discussed in [110,111]. In this model, a ‘‘Planck brane’’ and a ‘‘TeV brane’’ are added to the $\text{AdS}_5 \times S^5$ spacetime with a dual CFT. The ‘‘Planck brane’’ makes a UV cutoff hence adds a $(3 + 1)$ -dimensional gravity; the ‘‘TeV brane’’ makes an IR cutoff, and the standard model fields in it are understood as bound states out of the strong interacting CFT [114]. When at finite temperature, to make a lower free energy, the low temperature phase is as in the RS I model, but the high temperature phase favors an AdS-Schwarzschild solution (duals to the free CFT gas); hence, our universe should suffer a phase transition at some T_c lower than the Fermi scale. To ensure that the phase transition is completed thus for avoiding an empty universe, we need a strong upper bound for N_c of the dual CFT field. This model has already been discussed in Sec. III C 1, where we pointed out that an upper limit of N_c may be universal for some large- N_c theories which suffer some phase transitions.

The phase transition of an AdS/CFT model, in which a $(2 + 1)$ -dimensional field theory is dual to some (confined) AdS soliton or some (deconfined) black 3-brane metric compactified in a brane dimension, is discussed in [115]. The supercooling and the rapid reheating (hadronization) after it, are considered. Notwithstanding, in the large- N_c limit, the slowly hadronized phase at the temperature T_{dec} do not happen in their model. To begin at some supercooling temperature $T_0 > 0$, the residual deconfined regions after the phase transition still hold the energy portion larger than $1/4$. In that model, the supercooling scale is given by hand, and a lower limit $T_0 = 0$ ($\Delta = 1$) is considered. Comparing to that work, what we do in this paper is calculating Δ explicitly within some physical environments (what we use is the cosmological QCD phase transition). We use some AdS/CFT models more pertinent to the $(3 + 1)$ -dimensional QCD than theirs.

In addition, an interesting relation between the KSS bound and strange quark stars, is shown in [116]. The authors argued that, the surface of quark stars at the temperature $T \sim 80$ MeV, has already saturated the KSS bound.

The question which parallels to the topic we discussed in this paper, is how the RHIC results of strong interacting QGP and the AdS/CFT correspondence can affect the research of neutron stars and quark stars. The difference is that the deconfined QGP in quark stars is mainly caused by its high chemical potential, rather than caused by their high temperature in RHIC or the early universe. A lot of AdS/CFT models for finite chemical potential have already been constructed; although just as in the finite temperature case, they are mainly studied in the large- N_c limit. We will leave these issues to the follow-up studies.

ACKNOWLEDGMENTS

I would like to thank Ofer Aharony, Oleg Andreev, Thomas Cohen, Joshua Erlich, Itzhak Fouxon, Umur Gürsoy, Christopher Herzog, Keijo Kajantie, Joseph Kapusta, David Mateos, Berndt Müller, Robert Myers, Francesco Nitti, Matthew Roberts, Shigeki Sugimoto and Xin-Nian Wang for helpful discussions of issues related to this paper, and Gang Chen for organizing the folk AdS/CFT seminars. Darren Shih read the manuscript and gave me some advice and suggestions.

-
- [1] D. J. Schwarz, *Ann. Phys. (Leipzig)* **12**, 220 (2003).
 [2] D. Boyanovsky, H. J. de Vega, and D. J. Schwarz, *Annu. Rev. Nucl. Part. Sci.* **56**, 441 (2006).
 [3] O. Aharony, S. S. Gubser, J. M. Maldacena, H. Ooguri, and Y. Oz, *Phys. Rep.* **323**, 183 (2000).
 [4] J. M. Maldacena, *Adv. Theor. Math. Phys.* **2**, 231 (1998).

- [5] K. Peeters and M. Zamaklar, *Eur. Phys. J. Special Topics* **152**, 113 (2007).
 [6] D. Mateos, *Classical Quantum Gravity* **24**, S713 (2007).
 [7] M. Gyulassy and L. McLerran, *Nucl. Phys.* **A750**, 30 (2005).
 [8] D. Teaney, *Phys. Rev. C* **68**, 034913 (2003).

- [9] E. Shuryak, *Prog. Part. Nucl. Phys.* **53**, 273 (2004).
- [10] E. V. Shuryak, *Nucl. Phys.* **A750**, 64 (2005).
- [11] A. Chodos, R. L. Jaffe, K. Johnson, C. B. Thorn, and V. F. Weisskopf, *Phys. Rev. D* **9**, 3471 (1974).
- [12] T. A. DeGrand, R. L. Jaffe, K. Johnson, and J. E. Kiskis, *Phys. Rev. D* **12**, 2060 (1975).
- [13] J. D. Bekenstein, *Phys. Rev. D* **7**, 2333 (1973).
- [14] S. S. Gubser, I. R. Klebanov, and A. W. Peet, *Phys. Rev. D* **54**, 3915 (1996).
- [15] E. Witten, *Adv. Theor. Math. Phys.* **2**, 505 (1998).
- [16] S. S. Gubser, I. R. Klebanov, and A. A. Tseytlin, *Nucl. Phys.* **B534**, 202 (1998).
- [17] G. Policastro, D. T. Son, and A. O. Starinets, *J. High Energy Phys.* 12 (2002) 054.
- [18] S. S. Gubser, *Phys. Rev. D* **63**, 084017 (2001).
- [19] C.-j. Kim and S.-J. Rey, *Nucl. Phys.* **B564**, 430 (2000).
- [20] A. Nieto and M. H. G. Tytgat, *arXiv:hep-th/9906147*.
- [21] S. W. Hawking and D. N. Page, *Commun. Math. Phys.* **87**, 577 (1983).
- [22] S. S. Gubser and A. Nellore, *Phys. Rev. D* **78**, 086007 (2008).
- [23] S. S. Gubser, A. Nellore, S. S. Pufu, and F. D. Rocha, *Phys. Rev. Lett.* **101**, 131601 (2008).
- [24] S. S. Gubser, S. S. Pufu, and F. D. Rocha, *J. High Energy Phys.* 08 (2008) 085.
- [25] A. Karch and L. Randall, *J. High Energy Phys.* 06 (2001) 063.
- [26] A. Karch and E. Katz, *J. High Energy Phys.* 06 (2002) 043.
- [27] J. Erlich, E. Katz, D. T. Son, and M. A. Stephanov, *Phys. Rev. Lett.* **95**, 261602 (2005).
- [28] L. Da Rold and A. Pomarol, *Nucl. Phys.* **B721**, 79 (2005).
- [29] A. Karch, E. Katz, D. T. Son, and M. A. Stephanov, *Phys. Rev. D* **74**, 015005 (2006).
- [30] J. Babington, J. Erdmenger, N. J. Evans, Z. Guralnik, and I. Kirsch, *Phys. Rev. D* **69**, 066007 (2004).
- [31] I. Kirsch, *Fortschr. Phys.* **52**, 727 (2004).
- [32] K. Ghoroku, T. Sakaguchi, N. Uekusa, and M. Yahiro, *Phys. Rev. D* **71**, 106002 (2005).
- [33] R. Apreda, J. Erdmenger, N. Evans, and Z. Guralnik, *Phys. Rev. D* **71**, 126002 (2005).
- [34] T. Sakai and S. Sugimoto, *Prog. Theor. Phys.* **113**, 843 (2005).
- [35] T. Sakai and S. Sugimoto, *Prog. Theor. Phys.* **114**, 1083 (2005).
- [36] R. D. Pisarski, *Phys. Rev. D* **74**, 121703(R) (2006).
- [37] B. Lucini, M. Teper, and U. Wenger, *J. High Energy Phys.* 02 (2005) 033.
- [38] C. P. Herzog, *Phys. Rev. Lett.* **98**, 091601 (2007).
- [39] C. A. B. Bayona, H. Boschi-Filho, N. R. F. Braga, and L. A. P. Zayas, *Phys. Rev. D* **77**, 046002 (2008).
- [40] R.-G. Cai and J. P. Shock, *J. High Energy Phys.* 08 (2007) 095.
- [41] O. Andreev, *Phys. Rev. D* **76**, 087702 (2007).
- [42] K. Kajantie, T. Tahkokallio, and J.-T. Yee, *J. High Energy Phys.* 01 (2007) 019.
- [43] N. Evans and E. Threlfall, *arXiv:0805.0956*.
- [44] D. Mateos, R. C. Myers, and R. M. Thomson, *Phys. Rev. Lett.* **97**, 091601 (2006).
- [45] D. Mateos, R. C. Myers, and R. M. Thomson, *J. High Energy Phys.* 05 (2007) 067.
- [46] O. Aharony, J. Sonnenschein, and S. Yankielowicz, *Ann. Phys. (Leipzig)* **322**, 1420 (2007).
- [47] V. Mazu and J. Sonnenschein, *J. High Energy Phys.* 06 (2008) 091.
- [48] P. Benincasa and A. Buchel, *Phys. Lett. B* **640**, 108 (2006).
- [49] U. Gursoy and E. Kiritsis, *J. High Energy Phys.* 02 (2008) 032.
- [50] U. Gursoy, E. Kiritsis, and F. Nitti, *J. High Energy Phys.* 02 (2008) 019.
- [51] U. Gursoy, E. Kiritsis, L. Mazzanti, and F. Nitti, *Phys. Rev. Lett.* **101**, 181601 (2008).
- [52] U. Gursoy, E. Kiritsis, L. Mazzanti, and F. Nitti, *arXiv:0812.0792*.
- [53] Our EoS's agree with [22] qualitatively, and can catch all the expected limits; however, it has some small quantitative divergences rising from the numerical trickings. These divergences can affect the critical parameters we choose for the second order phase transition, but will not affect the main results of our discussions.
- [54] E. Farhi and R. L. Jaffe, *Phys. Rev. D* **30**, 2379 (1984).
- [55] G. Policastro, D. T. Son, and A. O. Starinets, *Phys. Rev. Lett.* **87**, 081601 (2001).
- [56] G. Policastro, D. T. Son, and A. O. Starinets, *J. High Energy Phys.* 09 (2002) 043.
- [57] P. Kovtun, D. T. Son, and A. O. Starinets, *J. High Energy Phys.* 10 (2003) 064.
- [58] A. Buchel and J. T. Liu, *Phys. Rev. Lett.* **93**, 090602 (2004).
- [59] A. Buchel, J. T. Liu, and A. O. Starinets, *Nucl. Phys.* **B707**, 56 (2005).
- [60] P. Benincasa and A. Buchel, *J. High Energy Phys.* 01 (2006) 103.
- [61] S. C. Huot, S. Jeon, and G. D. Moore, *Phys. Rev. Lett.* **98**, 172303 (2007).
- [62] J. Mas and J. Tarrío, *J. High Energy Phys.* 05 (2007) 036.
- [63] D. Mateos, R. C. Myers, and R. M. Thomson, *Phys. Rev. Lett.* **98**, 101601 (2007).
- [64] P. K. Kovtun, D. T. Son, and A. O. Starinets, *Phys. Rev. Lett.* **94**, 111601 (2005).
- [65] A. Buchel, *Phys. Lett. B* **663**, 286 (2008).
- [66] I. Fouxon, G. Betschart, and J. D. Bekenstein, *Phys. Rev. D* **77**, 024016 (2008).
- [67] T. D. Cohen, *Phys. Rev. Lett.* **99**, 021602 (2007).
- [68] D. T. Son, *Phys. Rev. Lett.* **100**, 029101 (2008).
- [69] T. D. Cohen, *Phys. Rev. Lett.* **100**, 029102 (2008).
- [70] A. Cherman, T. D. Cohen, and P. M. Hohler, *J. High Energy Phys.* 02 (2008) 026.
- [71] Y. Kats and P. Petrov, *J. High Energy Phys.* 01 (2009) 044.
- [72] M. Brigante, H. Liu, R. C. Myers, S. Shenker, and S. Yaida, *Phys. Rev. D* **77**, 126006 (2008).
- [73] M. Brigante, H. Liu, R. C. Myers, S. Shenker, and S. Yaida, *Phys. Rev. Lett.* **100**, 191601 (2008).
- [74] S. Gavin and M. Abdel-Aziz, *Phys. Rev. Lett.* **97**, 162302 (2006).
- [75] A. Majumder, B. Muller, and X.-N. Wang, *Phys. Rev. Lett.* **99**, 192301 (2007).
- [76] J. I. Kapusta and T. Springer, *Phys. Rev. D* **78**, 066017 (2008).
- [77] T. Hirano and M. Gyulassy, *Nucl. Phys.* **A769**, 71 (2006).

- [78] P. Arnold, G. D. Moore, and L. G. Yaffe, *J. High Energy Phys.* **11** (2000) 001.
- [79] D. Kharzeev and K. Tuchin, *J. High Energy Phys.* **09** (2008) 093.
- [80] H. B. Meyer, *Phys. Rev. Lett.* **100**, 162001 (2008).
- [81] F. Karsch, D. Kharzeev, and K. Tuchin, *Phys. Lett. B* **663**, 217 (2008).
- [82] O. Aharony, S. Minwalla, and T. Wiseman, *Classical Quantum Gravity* **23**, 2171 (2006).
- [83] H. Nastase, arXiv:hep-th/0501068.
- [84] E. Shuryak, S.-J. Sin, and I. Zahed, *J. Korean Phys. Soc.* **50**, 384 (2007).
- [85] Y. Iwasaki, K. Kanaya, L. Karkkainen, K. Rummukainen, and T. Yoshie, *Phys. Rev. D* **49**, 3540 (1994).
- [86] B. Beinlich, F. Karsch, and A. Peikert, *Phys. Lett. B* **390**, 268 (1997).
- [87] M. S. Berger and R. L. Jaffe, *Phys. Rev. C* **35**, 213 (1987).
- [88] T. A. DeGrand and K. Kajantie, *Phys. Lett. B* **147**, 273 (1984).
- [89] K. Kajantie, *Phys. Lett. B* **285**, 331 (1992).
- [90] P. J. Steinhardt, *Phys. Rev. D* **25**, 2074 (1982).
- [91] M. Gyulassy, K. Kajantie, H. Kurki-Suonio, and L. D. McLerran, *Nucl. Phys.* **B237**, 477 (1984).
- [92] J. Ignatius, K. Kajantie, H. Kurki-Suonio, and M. Laine, *Phys. Rev. D* **49**, 3854 (1994).
- [93] H. Kurki-Suonio, *Nucl. Phys.* **B255**, 231 (1985).
- [94] C. J. Hogan, *Phys. Lett. B* **133**, 172 (1983).
- [95] G. M. Fuller, G. J. Mathews, and C. R. Alcock, *Phys. Rev. D* **37**, 1380 (1988).
- [96] B. S. Meyer, C. R. Alcock, G. J. Mathews, and G. M. Fuller, *Phys. Rev. D* **43**, 1079 (1991).
- [97] J. Ignatius, K. Kajantie, H. Kurki-Suonio, and M. Laine, *Phys. Rev. D* **50**, 3738 (1994).
- [98] M. B. Christiansen and J. Madsen, *Phys. Rev. D* **53**, 5446 (1996).
- [99] J. H. Applegate and C. J. Hogan, *Phys. Rev. D* **31**, 3037 (1985).
- [100] E. Witten, *Phys. Rev. D* **30**, 272 (1984).
- [101] K. Kajantie and H. Kurki-Suonio, *Phys. Rev. D* **34**, 1719 (1986).
- [102] J. Ignatius and D. J. Schwarz, *Phys. Rev. Lett.* **86**, 2216 (2001).
- [103] L. P. Csernai and J. I. Kapusta, *Phys. Rev. D* **46**, 1379 (1992).
- [104] M. Cheng *et al.*, *Phys. Rev. D* **74**, 054507 (2006).
- [105] J. C. Miller and O. Pantano, *Phys. Rev. D* **40**, 1789 (1989).
- [106] J. C. Miller and O. Pantano, *Phys. Rev. D* **42**, 3334 (1990).
- [107] A. H. Guth and S. H. H. Tye, *Phys. Rev. Lett.* **44**, 631 (1980).
- [108] A. H. Guth and E. J. Weinberg, *Phys. Rev. D* **23**, 876 (1981).
- [109] J. I. Kapusta, arXiv:astro-ph/0101516.
- [110] P. Creminelli, A. Nicolis, and R. Rattazzi, *J. High Energy Phys.* **03** (2002) 051.
- [111] J. Kaplan, P. C. Schuster, and N. Toro, arXiv:hep-ph/0609012.
- [112] Z. Fodor and S. D. Katz, *J. High Energy Phys.* **04** (2004) 050.
- [113] C. Bernard *et al.* (MILC), *Phys. Rev. D* **71**, 034504 (2005).
- [114] N. Arkani-Hamed, M. Porrati, and L. Randall, *J. High Energy Phys.* **08** (2001) 017.
- [115] G. T. Horowitz and M. M. Roberts, *J. High Energy Phys.* **02** (2007) 076.
- [116] M. Bagchi *et al.*, *Phys. Lett. B* **666**, 145 (2008).
- [117] F. Karsch, E. Laermann, and A. Peikert, *Phys. Lett. B* **478**, 447 (2000).
- [118] M. Cheng *et al.*, *Phys. Rev. D* **77**, 014511 (2008).
- [119] O. Kaczmarek, F. Karsch, F. Zantow, and P. Petreczky, *Phys. Rev. D* **70**, 074505 (2004).